

Traffic-Aware Optimal Multi-Beam Resource Allocation in 5G Networks Impaired by Rain and Foliage

Tushar Bose^{ID}, Nilesh Chatur^{ID}, *Student Member, IEEE*, Mithun Mukherjee^{ID}, *Senior Member, IEEE*, Sandeep Verma^{ID}, *Senior Member, IEEE*, and Aneek Adhya^{ID}, *Member, IEEE*

Abstract—In this letter, we study a traffic-aware multi-beam optimal resource allocation strategy for fixed home users who are serviced through the utilization of simultaneous multiple beams generated by next-generation node B (gNB). The strategy takes into account the effects of rain and foliage attenuation. We propose a graphical methodology that is combined with a closed-form expression to compute the optimal coverage radius of gNB. Afterwards, the k-means clustering algorithm is utilized to determine an optimal location for the gNB. In this study, we also present an approach that employs non-linear programming (NLP) to allocate power and bandwidth among individual beams, with an objective of satisfying the traffic requirements of each user. From the results, it is evident that our proposed approach exhibits superior performance in scenarios characterized by rain and foliage attenuation, in comparison to alternatives relying on genetic algorithms and surrogate optimization approaches.

Index Terms—Fifth generation (5G), foliage attenuation, millimeter wave, multi-beam resource allocation, rain attenuation.

I. INTRODUCTION

THE proliferation of cutting-edge technologies such as augmented reality and virtual reality has resulted in a substantial increase in the necessity of data traffic throughout the network. The substantial accessibility of bandwidth in millimeter wave (mm-wave) frequency bands enables mm-wave to be a viable option for addressing the growing data demands of the fifth-generation (5G) network. However, *mm-wave bands incur a high path loss and are severely affected by rain and foliage attenuation*. The aforementioned propagation challenges of mm-wave are generally mitigated by the use of beamforming and small cells. In this letter, we focus on beamforming in small cells, achieved through uniform planar array (UPA) installed at the 5G next-generation node B (gNB) by generating multiple beams to concurrently serve users in different spatial locations.

Several studies have examined *rain and foliage attenuation in mm-wave frequency bands* through a combination of

Manuscript received 24 December 2023; accepted 10 January 2024. Date of publication 22 January 2024; date of current version 12 March 2024. This work is partially supported by the Ministry of Electronics and Information Technology (MeitY), Govt. of India under the project “Next Generation Wireless Research and Standardization on 5G and Beyond” in IIT Kharagpur. The associate editor coordinating the review of this letter and approving it for publication was F. Liu. (*Corresponding author: Aneek Adhya*)

Tushar Bose, Nilesh Chatur, and Aneek Adhya are with the G. S. Sanyal School of Telecommunication, IIT Kharagpur, Kharagpur 721302, India (e-mail: btushar@kgpian.iitkgp.ac.in; nileshchatur@gssst.iitkgp.ac.in; aneek@gssst.iitkgp.ac.in).

Mithun Mukherjee is with the Department of Computer and Communication Engineering, Khalifa University, Abu Dhabi, United Arab Emirates (e-mail: mithun.mukherjee@ku.ac.ae).

Sandeep Verma is with the Bharti School of Telecommunication Technology and Management, IIT Delhi, Delhi 110016, India (e-mail: sandeepverma@ieee.org).

Digital Object Identifier 10.1109/LCOMM.2024.3357174

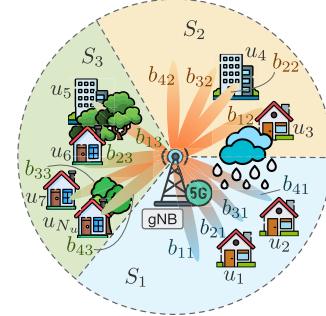


Fig. 1. System model. The fixed home users are served simultaneously through multiple beams in the presence of rain and foliage attenuation.

experimental measurement-based approaches ([1], [2]), theoretical analyses ([3], [4]), and ray-tracing-based simulations ([5]). For example, Han and Duan [1] carried out mm-wave measurements in Beijing, China, and studied the impact of rain and other atmospheric parameters on mm-wave at 23/25/28/38 GHz. Zheng et al. [2] presented a field experiment of E-band mm-wave link in Nanjing, China to study rain-induced attenuation. In [3], the impact of rainfall and sand dust storms on the performance of mm-wave at 24/28/38/75 GHz was analyzed. Further, Barb et al. [4] carried out theoretical analysis and simulations to study the vegetation loss in the 28 GHz mm-wave band. Ray-tracing has been adopted in [5] to study the impact of rainfall in mm-wave. Wang and Wong [6] introduce a joint resource block allocation and beamforming method for *beam resource allocation* in 5G to support enhanced mobile broadband and ultra-reliable low-latency communication. In another parallel work, Yu et al. [7] investigate a deep learning-based *beam resource allocation* method for 5G broadband services.

Studies on rain and foliage attenuation relying on experiments ([1], [2]) require resource-intensive field measurements. Ray tracing ([5]) is computationally expensive as they require solving complex electromagnetic (EM) equations. In theoretical studies for rain and foliage attenuation ([3], [4]), multi-beam resource allocation was not widely considered. On the other hand, pertaining to multi-beam resource allocation ([6], [7]), rain and foliage effects have not been considered. Our work introduces an optimization framework to determine optimal gNB coverage radius, gNB location, and multi-beam resource allocation, considering rain and foliage attenuation. This optimization-based approach offers enhanced versatility without delving into extensive fieldwork or complex EM equation analysis before 5G small-cell deployment. The main contributions are summarized as follows:

- We propose an optimization method to obtain the optimal coverage radius of a gNB satisfying the

quality-of-service (QoS) demands of all users inside a small cell. Specifically, we derive the optimum coverage radius by considering multiple factors, such as free-space, rain attenuation, and foliage attenuation, utilizing a revolutionary graphical approach. Additionally, we provide the closed-form equation for the optimal coverage radius, accounting for both free-space and foliage attenuation.

- We determine the optimal location of gNB by utilizing k-means clustering algorithm of the unsupervised machine learning (ML) framework. Our proposed approach outperforms the genetic algorithm and surrogate optimization-based approaches (in terms of the number of users served) for rain and foliage attenuation scenarios. Finally, we propose a non-linear programming (NLP)-based optimization framework for optimum multi-beam resource (particularly focusing on power- and bandwidth-per-beam) allocation under rain and foliage attenuation.

II. SYSTEM MODEL

Fig. 1 illustrates the system model wherein fixed home users within a small geographical area are served via a small cell gNB. The user set is $U = \{u_1, u_2, \dots, u_i, \dots, u_{N_u}\}$, with N_u number of users wherein u_i denotes the i th user. The x and y coordinates of u_i are represented as x_{u_i} and y_{u_i} respectively. The gNB is equipped with three UPAs, and each UPA serves a disjoint sector of 120° . The k th sector is denoted as S_k and $k \in \{1, 2, 3\}$. Each UPA generates N_b simultaneous beams to serve each sector. The set of beams available for S_k is denoted as $B^{S_k} = [b_{1k}, b_{2k}, \dots, b_{jk}, \dots, b_{N_b k}]$, where $j = 1, 2, \dots, N_b$ and b_{jk} is the j th beam of the k th sector. The total power and bandwidth available for each sector are denoted as P_t and \mathcal{W}_t , respectively. The data rate demand for users is represented as $\{D_{u_1}, D_{u_2}, \dots, D_{u_i}, \dots, D_{u_{N_u}}\}$. In the proposed framework for traffic-aware multi-beam resource allocation, the initial step involves computation of the *optimal radius* of the gNB. Subsequently, the *optimal position* of the gNB is obtained using computational analysis. Using the radius and position of the gNB, the number of users served by the gNB is identified for different environmental impairments. Further, we formulate an NLP-based optimization model to determine the *optimal values for beam power and bandwidth incorporating the effects of rain and foliage attenuation*.

III. COMPUTATION OF OPTIMAL COVERAGE RADIUS OF GNB IN PRESENCE OF RAIN AND FOLIAGE ATTENUATION

A. Computation of Optimal Coverage Radius of gNB Considering Free-Space Propagation Loss

The free-space propagation path loss is expressed as [8]

$$\text{PL}^f(r) = \text{PL}_0 + 10 n_p \log_{10} \left(\sqrt{(h_g - h_u)^2 + r^2} \right), \quad (1)$$

where n_p is the model parameter representing the path loss exponent, h_g and h_u are the antenna heights of the gNB and user equipment, respectively. The radius of gNB is denoted by r and PL_0 is the free-space path loss at a transmitter-receiver separation distance of 1 m and is expressed as $\text{PL}_0 = 20 \log_{10}(4\pi f/c)$, where f is the operating frequency (in Hz) and c is the speed of light. The received signal power is expressed as $P^{\text{rec}}(r) = P^t - \text{PL}^f(r)$, where $P^{\text{rec}}(r)$ is the

received signal power at distance r from the gNB and P^t is the transmitted power from the gNB. To ensure the desired QoS over the entire small cell of the gNB, the received signal power at distance r should be greater than a predefined threshold denoted as P_{\min} , i.e., $P^{\text{rec}}(r) \geq P_{\min}$, or $P^t - \text{PL}^f(r) \geq P_{\min}$.

Therefore, the optimization problem for maximizing the coverage radius of the gNB considering free-space propagation loss is formulated as

$$\max_r \quad r \quad (2a)$$

$$\text{s.t. } P^t - \text{PL}^f(r) \geq P_{\min} \text{ and } r \geq 0. \quad (2b)$$

Now, we derive the closed-form expression for the maximum coverage radius of gNB, ensuring the desired QoS and considering the free-space propagation loss as R_f^* .

$$R_f^* = \left[2^{\frac{P^t - P_{\min}}{5n_p} - \frac{8}{n_p}} 5^{\frac{P^t - P_{\min}}{5n_p}} c^{\frac{4}{n_p}} f^{\frac{-4}{n_p}} \pi^{\frac{-4}{n_p}} + 2h_g h_u - h_g^2 - h_u^2 \right]^{\frac{1}{2}}. \quad (3)$$

B. Computation of Optimal Coverage Radius of gNB in Presence of Rain Attenuation

Typically, the rain attenuation in dB/km can be expressed as [9] $\gamma_{\text{rain}} = KR^\alpha$, where R is the rate of rainfall expressed in mm/hr. K and α are the frequency-dependent constants, respectively expressed as

$$\log_{10} K = \sum_{j=1}^{j=4} a_j e^{-\frac{\log_{10} f_{\text{GHz}} - b_j}{c_j}} + m_k \log_{10} f_{\text{GHz}} + c_k, \quad (4)$$

$$\alpha = \sum_{j=1}^{j=5} a_j e^{-\frac{\log_{10} f_{\text{GHz}} - b_j}{c_j}} + m_\alpha \log_{10} f_{\text{GHz}} + c_\alpha, \quad (5)$$

where f_{GHz} is the operating frequency in GHz, and a_j , b_j , c_j , m_k , m_α , c_k , and c_α are constants [9]. We rewrite the optimization problem (2a) to compute the optimal coverage radius of gNB in the presence of rain attenuation as

$$\max_r \quad r \quad (6a)$$

$$\text{s.t. } P^t - \text{PL}^f(r) - 0.001\gamma_{\text{rain}} \times r \geq P_{\min} \text{ and } r \geq 0. \quad (6b)$$

We solve the aforementioned optimization problem using graphical approach.

C. Computation of Optimal Coverage Radius of gNB in Presence of Foliage Attenuation

The foliage attenuation in dB is expressed as [4] $\gamma_{\text{foliage}} = 0.2 f_{\text{MHz}}^{0.3} \times d_f^{0.6}$, where f_{MHz} is the operating frequency in MHz and d_f is the depth of foliage. Thus, the optimization problem for maximizing the coverage radius of gNB in the presence of foliage attenuation can be formulated as

$$\max_r \quad r \quad (7a)$$

$$\text{s.t. } P^t - \text{PL}^f(r) - \gamma_{\text{foliage}} \geq P_{\min} \text{ and } r \geq 0. \quad (7b)$$

We further derive the closed-form relation for maximizing the coverage radius of gNB with foliage attenuation as R_{fo}^* .

$$R_{\text{fo}}^* = \left[2h_g h_u - h_g^2 - h_u^2 + c^{\frac{4}{n_p}} f^{\frac{-4}{n_p}} \times e^{\left(\frac{-10.1 - 0.09(d_f^{0.6})(f_{\text{MHz}}^{0.3}) - 0.4P_{\min} + 0.4P^t}{n_p} \right)} \right]^{\frac{1}{2}}. \quad (8)$$

IV. COMPUTATION OF OPTIMAL LOCATION OF gNB AND OPTIMAL MULTI-BEAM RESOURCE ALLOCATION

In this section, we discuss the method to determine the gNB's optimal location. Afterwards, we present the optimization framework for multi-beam resource allocation.

A. Computation of Optimal gNB Location

The optimization problem for computing the optimal gNB location utilizing the location information of users is stated as

$$\max \sum_{\forall u_i \in U} \tilde{u}_i \quad (9a)$$

$$\text{s.t. } \tilde{u}_i \in \{0, 1\} \quad (9b)$$

$$\tilde{u}_i \left((x_i - x_g)^2 + (y_i - y_g)^2 \right) \leq R_{\text{opt}} \quad \forall u_i \in U. \quad (9c)$$

The above objective function maximizes the number of users inside the coverage area of the gNB. Here, \tilde{u}_i is a binary decision variable; $\tilde{u}_i = 1$ if the i th user (i.e., u_i) is within the coverage of the gNB, and $\tilde{u}_i = 0$, otherwise. In constraint (9c), R_{opt} is the optimal coverage radius of gNB depending upon the propagation scenario, viz., free-space, rain attenuation, and foliage attenuation (as discussed in section III). The problem of computing the optimal location of gNB is non-polynomial hard. To address the aforementioned limitation, in this letter, we utilize k-means clustering algorithm (with $k = 1$) of the unsupervised ML framework to compute the optimal location of gNB [10]. Due to the association of users to a single cluster (gNB), i.e., $k = 1$, the objective function is a convex function [11]. Thus, the k-means algorithm identifies the optimal gNB location (centre point) that aligns with the users' distribution over the geographical area of interest.

B. Traffic Aware Multi-Beam Optimal Resource Allocation

We consider a UPA with N_x and N_y antenna elements in x and y directions with inter-element spacing of d_x and d_y , respectively. The UPA serves a sector of 120° by generating simultaneous multiple beams [12]. Now, the received power at user u_i is given as

$$\mathbf{P}_{b_{jk}}^{u_i} = P_{u_i}^k \|H_{u_i} W_{b_{jk}}\|_F^2 \quad \forall b_j \in B^{S_k}, \quad k = 1, 2, 3$$

$$b_{jk}^* = \underset{b_{jk}}{\text{Argmax}} \mathbf{P}_{b_{jk}}^{u_i}; \quad P_r^{u_i} = P_{u_i}^k \|H_{u_i} W_{b_{jk}^*}\|_F^2, \quad (10)$$

where $\mathbf{P}_{b_{jk}}^{u_i}$ is the power received at user u_i through beam b_{jk} , $P_{u_i}^k$ is the power allocated to user u_i of sector S_k , $W_{b_{jk}}$ is the beamforming vector of beam b_{jk} , and H_{u_i} is the mm-wave channel matrix for user u_i . H_{u_i} incorporates both the large-scale and small-scale fading effects. Following [13], the received power is computed using the framework of simultaneous beam generation, channel matrix, and the array response vector. The optimal beam for user u_i is b_{jk}^* and $\|\cdot\|_F$ denotes the Frobenius norm. The power received by user u_i through the optimal beam b_{jk}^* is denoted as $P_r^{u_i}$, and $W_{b_{jk}^*}$ is the beamforming vector corresponding to beam b_{jk}^* . Then, the NLP-based optimization framework for traffic-aware multi-beam optimum resource allocation problem for a sector S_k is modelled as

$$\min \sum_{\forall u_i \in S_k} (D_{u_i} - C_{u_i})^2 \quad (11a)$$

$$\text{s.t. } \sum_{\forall u_i \in S_k} P_{u_i}^k \leq \mathcal{P}_t \quad (11b)$$

$$\sum_{\forall u_i \in S_k} W_{u_i}^k \leq \mathcal{W}_t \quad (11c)$$

$$C_{u_i} \leq D_{u_i} \quad \forall u_i \in S_k \quad (11d)$$

$$(D_{u_i} - C_{u_i})^2 \leq \epsilon \quad \forall u_i \in S_k \quad (11e)$$

$$0 \leq P_{u_i}^k \leq \mathcal{P}_t \quad \forall u_i \in S_k \quad (11f)$$

$$0 \leq W_{u_i}^k \leq \mathcal{W}_t \quad \forall u_i \in S_k \quad (11g)$$

$$C_{u_i} = W_{u_i}^k \log_2 (1 + P_r^{u_i} / N_0) \quad (11h)$$

The above objective function aims to minimize the difference between the requested data rate (D_{u_i}) and the achieved data rate (C_{u_i}) of users. Specifically, (11a) minimizes the sum of squared error between D_{u_i} and C_{u_i} associated with sector S_k . In constraint (11b), $P_{u_i}^k$ is the power allocated to user u_i of sector S_k ; constraint (11b) guarantees that the power allocated to all the users of sector S_k is less than or equal to the total power available with a sector. In constraint (11c), $W_{u_i}^k$ is the bandwidth allocated to user u_i of sector S_k ; constraint (11c) guarantees that the total bandwidth allocated to all the users of sector S_k is less than or equal to the total bandwidth available in the sector. Constraint (11d) ensures that the capacity achieved is less than or equal to the requested data rate by a user. Constraint (11e) guarantees that the square of the difference between the requested data rate and the achieved data rate is less than or equal to the tolerance limit (ϵ). Constraints (11f) and (11g) define the bounds on the power and bandwidth of user u_i , respectively. Finally, equation (11h) gives the relation to obtain C_{u_i} , wherein N_0 denotes the noise power. The power (bandwidth) allocated to beam b_{jk} is the sum of the powers (bandwidths) allocated to u_i 's that are served by beam b_{jk} . In this letter, we utilize a trust region reflective (TRR)-based methodology, wherein the quadratic model of the Lagrangian function is computed to solve the NLP [14].

V. SIMULATION RESULTS AND DISCUSSIONS

We consider a rectangular area of $200 \times 200 \text{ m}^2$ with 22 uniformly distributed users. The simulation parameters are summarized in Table I. Fig. 2(a), 2(b), and 2(c) illustrate the details of the network deployment, i.e., the number of users covered, the optimal location of gNB, and the optimal coverage radius of gNB for rainfall rates of 10 mm/hr, 20 mm/hr, and 25 mm/hr respectively. Fig. 2(d), 2(e), and 2(f) illustrate the network deployment for foliage depths of 1m, 2 m, and 5 m respectively. The location of gNB is obtained through k-means clustering algorithm that converges for the maximum iterations of 100 or the convergence threshold of 10^{-4} . Fig. 3(a), 3(b), and 3(c) illustrate the coverage of users through simultaneous multiple beams for rainfall rates of 10 mm/hr, 20 mm/hr, and 25 mm/hr respectively. Fig. 3(d), 3(e), and 3(f) illustrate the coverage of users through simultaneous multiple beams for foliage depths of 1 m, 2 m, and 5 m, respectively. From Figs. 4(a) and 4(b), it is observed that the proposed k-means clustering for computing the optimal location of gNB can serve more users in the presence of rain and foliage as compared to genetic algorithm [15]- and surrogate optimization [16]-based

TABLE I
SIMULATION PARAMETERS

Simulation parameters	Values
Operating frequency (f)	28 GHz
Antenna height of gNB (h_g)	25 m
Antenna height of users (h_u)	1.5 m
Dimension of UPA ($N_x \times N_y$)	16 × 16
Inter-element spacing of antenna elements in x - and y -direction (d_x, d_y)	$c/2f$
Number of beams per sector (N_b)	8
Transmitted power from gNB (P^t)	43 dBm
Received signal power threshold (P_{\min})	-75 dBm
Maximum power available per sector (\mathcal{P}_t)	43 dBm
Maximum bandwidth available per sector (\mathcal{W}_t)	20 MHz
Noise power (N_0)	-120 dBm
Tolerance limit (ϵ)	10^{-3}

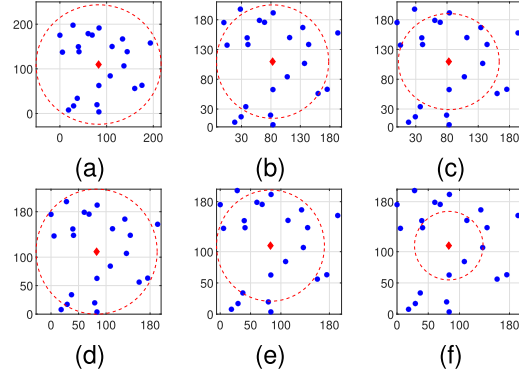


Fig. 2. Network deployment, with the maximum number of users covered, the optimal location of gNB, and the optimal coverage radius of gNB for different rainfall rates (R) and foliage depths (d_f). The blue dots represent the fixed home user locations, the red diamond represents the optimal gNB location, and the red dotted circle represents the optimal gNB coverage radius with (a) $R = 10$ mm/hr, (b) $R = 20$ mm/hr, (c) $R = 25$ mm/hr, (d) $d_f = 1$ m, (e) $d_f = 2$ m, and (f) $d_f = 5$ m.

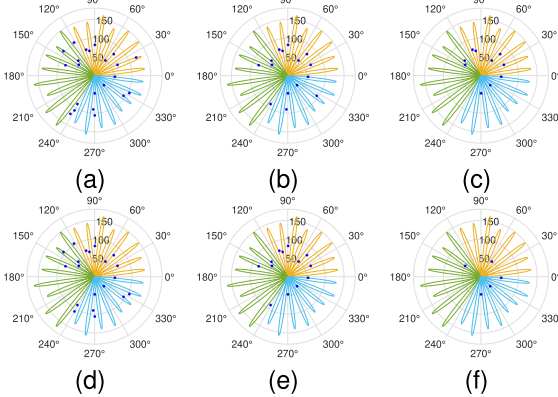


Fig. 3. User coverage (represented using polar plot) by simultaneous multiple beams for different rainfall rates (R) and foliage depths (d_f). The blue dots represent the user locations. Orange, green, and blue beams cover the first, second, and third sector respectively, where (a) $R = 10$ mm/hr, (b) $R = 20$ mm/hr, (c) $R = 25$ mm hr, (d) $d_f = 1$ m, (e) $d_f = 2$ m, and (f) $d_f = 5$ m.

approaches. In the genetic algorithm to determine the optimal location of gNB, we consider population size as 200, the maximum number of generations as 2000, crossover fraction as 0.85, and function tolerance as 10^{-6} . While, for surrogate optimization, we consider the maximum number of function evaluations as 50, the minimum number of surrogate points as 20, the batch update interval as 1, and the minimum sample distance as 10^{-6} . Compared to genetic algorithm, the proposed method offers an average performance improvement of 12.12% for rain attenuation and 15.58% for foliage

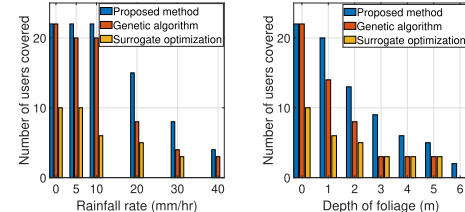


Fig. 4. Number of users supported in various rainfall rates and foliage depths.

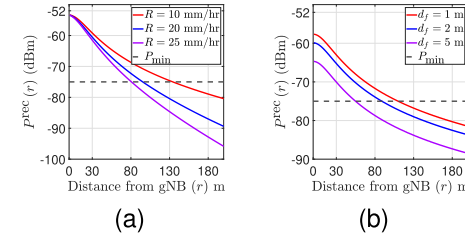


Fig. 5. Computation of the optimal gNB radius using the graphical methodology for different (a) rainfall rates and (b) foliage depths.

attenuation. As compared to surrogate optimization, we obtain a performance improvement of 44.69% for rain attenuation and 30.51% for foliage attenuation.

Insights: The genetic and surrogate optimization strategies do not adequately account for the spatial distribution of users. On the one hand, the evolutionary algorithm generally explores a vast solution space by evaluating numerous locations inside the given area. Therefore, the effectiveness of identifying the ideal gNB placement is limited by the vast solution space. On the other hand, developing an appropriate surrogate model that incorporates the spatial distribution of users poses a significant challenge when dealing with a limited geographical area. The surrogate model that has been developed exhibits limitations in accurately representing the precise spatial distribution of users, leading to a less reliable solution. Interestingly, by the utilization of the spatial distribution of users in our proposed approach based on k-means, we can determine the optimal placement of the gNB. This placement results in a higher number of users being served in comparison to approaches that rely on genetic and surrogate optimization methods.

Optimal gNB radius: Figs. 5(a) and 5(b) illustrate the outcome of the proposed graphical approach to find the optimal gNB radius for various rainfall rates and foliage depths, respectively. The intersection points of the received signal power $P^{\text{rec}}(r)$ with P_{\min} gives the optimal coverage radius of gNB ensuring the desired QoS in terms of user data rate requirements. From the figures, it is observed that as R and d_f increases the optimum coverage radius of the gNB decreases, owing to the increase in losses due to rain and foliage attenuation. Moreover, we show optimal coverage radius of gNB for different rainfall rates and foliage depths in Fig. 6(a) and 6(b), respectively. From the figures, it is observed that there is a significant decrease in the optimal coverage radius of the gNB as the foliage depth increases. In contrast, the decrease in the optimal radius is more gradual as the rainfall rate increases. Based on the aforementioned tendencies, it may be argued that foliage has a more significant impact on mm-waves than rain attenuation.

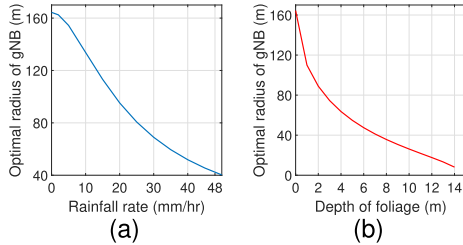


Fig. 6. Optimal coverage radius of gNB for different (a) rainfall rates and (b) foliage depths.

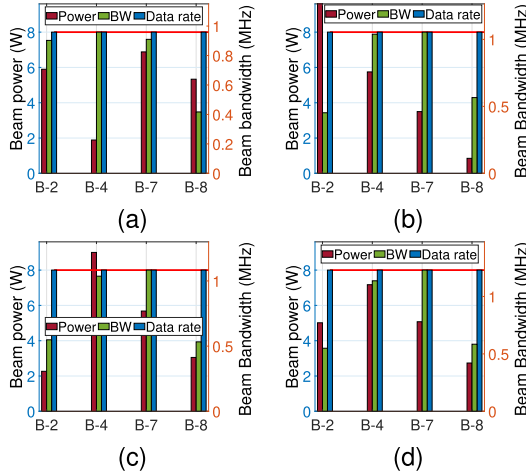


Fig. 7. Optimal power, bandwidth allocation, and achieved average data rate for beams of sector 1. We denote B-2, B-4, B-7, and B-8 as the 2nd, 4th, 7th, and 8th beam, respectively. The red straight line represents the target data rate: (a) $R = 5 \text{ mm/hr}$, (b) $R = 15 \text{ mm/hr}$, (c) $d_f = 1 \text{ m}$, and (d) $d_f = 2 \text{ m}$.

Optimal power and bandwidth allocation and average data rate: We set the requested data rate of users as $D_{ui} = 8 \text{ Mbps}$. We execute TRR algorithm considering the values of initial trust region, maximum trust region, maximum number of iterations, and objective tolerance as 0.1, 1, 100, and 10^{-6} , respectively [14]. We depict the optimal power and bandwidth allocation to the beams of the first sector (as a part of illustration, we take orange beams of Fig. 3) for different rainfall rates and foliage depths with the NLP-based framework in Fig. 7. The NLP-based framework assigns zero power and bandwidth to the beams, which do not serve any user (Fig. 3). Moreover, we show the achieved average data rate of the users supported by the individual (selected) beams in the figure. We refer the achieved average data rate of the beam as the average of the supported data rate of the users served by the given beam. Fig. 7 shows that the proposed resource allocation scheme assigns different values of optimal beam power and beam bandwidth for different levels of environmental impairments (i.e., various rainfall rates and foliage depths). Furthermore, the resource allocation scheme adheres to power (\mathcal{P}_t) and bandwidth (\mathcal{W}_t) constraints for each level of environmental impairment.

VI. CONCLUSION AND FUTURE SCOPE

In this study, we have demonstrated a framework for optimal traffic-aware 5G multi-beam resource allocation in the presence of rain and foliage attenuation. Our proposed NLP-based framework effectively allocates power and bandwidth to each beam serving a group of spatially separated users. From the results, it is observed that our k-means-based

methodology supports more users in a given geographical area for various rainfall rates and foliage depths as compared to genetic and surrogate-based approaches. Interestingly, our proposed methodology demonstrates an average performance improvement of 12.12% and 15.58% in terms of the total number of users served over the genetic algorithm for different rainfall rates and foliage depths. Further, an average performance improvement of 30.51% and 44.69% was observed over the surrogate optimization for different rainfall rates and foliage depths, respectively. In future, we plan to include other impairments of mm-waves, such as atmospheric absorption, material penetration, and blockages for efficient network design and resource allocation for 5G and 6G networks.

REFERENCES

- [1] C. Han and S. Duan, "Impact of atmospheric parameters on the propagated signal power of millimeter-wave bands based on real measurement data," *IEEE Access*, vol. 7, pp. 113626–113641, 2019.
- [2] S. Zheng et al., "The impact of rainfall on E-band millimeter-wave links in east China," in *Proc. 34th Gen. Assem. Sci. Symp. Int. Union Radio Sci. (URSI GASS)*, Aug. 2021, pp. 1–4.
- [3] M. Olyaei et al., "The effect of sand and dust storms (SDSs) and rain on the performance of cellular networks in the millimeter wave band," *IEEE Access*, vol. 11, pp. 69252–69262, 2023.
- [4] G. Barb, F. Danuti, M. A. Ouamri, and M. Otesteanu, "Analysis of vegetation and penetration losses in 5G mmWave communication systems," in *Proc. Int. Symp. Electron. Telecommun. (ISETC)*, Nov. 2022, pp. 1–5.
- [5] E. Hamiti and K. Gegaj, "Study of rain attenuation effects for 5G mm wave cellular communications in real scenarios," *J. Commun. Technol. Electron.*, vol. 66, no. S2, pp. S109–S117, Dec. 2021.
- [6] Z. Wang and V. W. S. Wong, "Joint resource block allocation and beamforming with mixed-numerology for eMBB and URLLC use cases," in *Proc. IEEE Global Commun. Conf. (GLOBECOM)*, Dec. 2021, pp. 1–6.
- [7] P. Yu, F. Zhou, X. Zhang, X. Qiu, M. Kadoc, and M. Cheriet, "Deep learning-based resource allocation for 5G broadband TV service," *IEEE Trans. Broadcast.*, vol. 66, no. 4, pp. 800–813, Dec. 2020.
- [8] P. Zhang, B. Yang, C. Yi, H. Wang, and X. You, "Measurement-based 5G millimeter-wave propagation characterization in vegetated suburban macrocell environments," *IEEE Trans. Antennas Propag.*, vol. 68, no. 7, pp. 5556–5567, Jul. 2020.
- [9] F. Norouzian et al., "Rain attenuation at millimeter wave and low-THz frequencies," *IEEE Trans. Antennas Propag.*, vol. 68, no. 1, pp. 421–431, Jan. 2020.
- [10] T. Bose, A. Suresh, O. J. Pandey, L. R. Cenkeramaddi, and R. M. Hegde, "Improving quality-of-service in cluster-based UAV-assisted edge networks," *IEEE Trans. Netw. Service Manage.*, vol. 19, no. 2, pp. 1903–1919, Jun. 2022.
- [11] T. V. Gruzdeva and A. V. Ushakov, "K-means clustering via a nonconvex optimization approach," in *Proc. Int. Conf. Math. Optim. Theory Oper. Res.* Cham, Switzerland: Springer, Jun. 2021, pp. 462–476.
- [12] R. M. Dreifuerst, R. W. Heath, and A. Yazdan, "Massive MIMO beam management in sub-6 GHz 5G NR," in *Proc. IEEE 95th Veh. Technol. Conf. (VTC-Spring)*, Jun. 2022, pp. 1–5.
- [13] I. A. Hemadeh, K. Satyanarayana, M. El-Hajjar, and L. Hanzo, "Millimeter-wave communications: Physical channel models, design considerations, antenna constructions, and link-budget," *IEEE Commun. Surveys Tuts.*, vol. 20, no. 2, pp. 870–913, 2nd Quart., 2018.
- [14] J. Liu, D. Wang, J. Liang, and Z. Mei, "Channel capacity optimization based on Riemannian trust region algorithm in IRS-aided communication system," *China Commun.*, vol. 19, no. 10, pp. 21–37, Oct. 2022.
- [15] Y. Sun, I. Silvestrov, and A. Bakulin, "Enhancing 3-D land seismic data using nonlinear beamforming based on the efficiency-improved genetic algorithm," *IEEE Trans. Evol. Comput.*, vol. 26, no. 5, pp. 1192–1199, Oct. 2022.
- [16] H. Tong, C. Huang, L. L. Minku, and X. Yao, "Surrogate models in evolutionary single-objective optimization: A new taxonomy and experimental study," *Inf. Sci.*, vol. 562, pp. 414–437, Jul. 2021.